Monatsh Chem (2015) 146:839–847
DOI 10.1007/s00706-015-1435-6

ORIGINAL PAPER

Electrochemical behavior of anthraquinone- and nitrophenyl-labeled deoxynucleoside triphosphates: a contribution to development of multipotential redox labeling of DNA

Pavlína Vidláková · Hana Pivoňková · Miroslav Fojta · Luděk Havran

Received: 5 December 2014 / Accepted: 2 February 2015 / Published online: 25 February 2015

Abstract Electrochemical properties of base-modified cytosine or 7-deazaadenine nucleoside triphosphates (dNTPs) bearing electrochemically active anthraquinone or 3-nitrophenyl moieties were studied using cyclic voltammetry with the hanging mercury drop electrode. The anthraquinone moiety in the dNTPs gives well-pronounced reversible quinone/hydroquinone redox signals around −0.40 V (against AglAgCl|3M KCl reference electrode), while the nitro group in 3-nitrophenyl exhibits irreversible reduction to hydroxylamine around −0.45 V that can be reversibly oxidized to corresponding nitroso compound close to 0.0 V. Both anthraquinone and hydroxylamine redox groups can be selectively switched off by further electrochemical transformation, depending on negative potential applied and composition of the background electrolyte. Results of this study suggest that both nucleobase and the conjugate label moiety influence remarkably the adsorbability and/or intermolecular interactions taking part at the electrode surface. The potential analytical utilization of these phenomena is discussed.

Graphical abstract

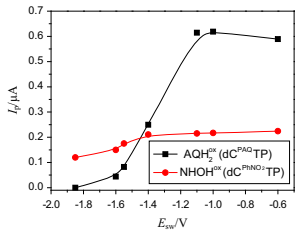

Keywords Nucleoside triphosphate · DNA labeling · DNA electrochemistry · Anthraquinone · Nitro compounds · Cyclic voltammetry

P. Vidláková · H. Pivoňková · M. Fojta · L. Havran (✉)
Institute of Biophysics, Academy of Sciences of the Czech Republic, v.v.i., Kralovopolska 135, 612 65 Brno, Czech Republic
e-mail: raven@ibp.cz

M. Fojta
Central European Institute of Technology, Masaryk University, Kamenice 753/5, 625 00 Brno, Czech Republic

Introduction

Labeling of nucleic acids (NA) by various electroactive tags is of broad interest to scientists in connection with the development of electrochemical methods and biosensors for NA analysis, such as analysis of nucleotide sequences or sensing of DNA damage (reviewed in [1–3]). Redox labels can be introduced into NA via chemical phosphoramidite-based synthesis of oligonucleotides, by chemical modification of natural NA components (such as thymine residues in DNA by osmium tetroxide reagents [4] or 3′-terminal ribose in RNA by six-valent osmium complexes [5]), or enzymatically using polymerases and labeled (deoxy)nucleoside triphosphates [(d)NTPs] as monomer substrates. The latter approach has proved especially efficient and versatile for the preparation of not only the redox-labeled DNA, but also DNA bearing fluorophores [6, 7] or chemically reactive groups for further chemical transformations on DNA [8, 9] or for bioconjugation with proteins

[10]. A number of modified dNTP bearing diverse electrochemically active moieties, such as ferrocene [11], organic nitrocompounds [12], [Ru/Os-(bpy)$_3$] complexes [13], anthraquinone [14], benzofurazane [15], methoxyphenol [16], phenylazide [8], and others (reviewed in [2, 17]), have been developed and applied. A combination of these labels (to encode different nucleotide sequences, or even each nucleobase with different tags being electrochemically reduced or oxidized at different potentials) allows parallel analysis of multiple nucleotide sequences [18], typing of sequence polymorphisms [12, 13], or a simple monitoring of the conversion of one redox tag to another, e.g., to probe interactions of the modified DNA with proteins [8].

Anthraquinone (AQ), as a moiety exhibiting well-pronounced reversible electrochemistry [19–21], has been utilized for redox labeling of biomolecules [22–24]. Derivatives of AQ linked via various tethers to nucleosides were used, for example, to study DNA-mediated charge transfer [25–27]. Base-modified cytosine and 7-deaza-adenine dNTPs bearing the AQ labels have recently been developed and used for polymerase synthesis of AQ-modified oligodeoxynucleotides, and utilization of the AQ tags for dual redox labeling of DNA in combination with earlier introduced nitrophenyl ($PhNO_2$) labels in simple model applications have been tested [14]. However, a more detailed study of electrochemical properties of oligodeoxyribonucleotides (ODNs) bearing AQ or $PhNO_2$ groups, or their combination, is to date missing. In this paper, we present a comparative study of base-modified AQ or $PhNO_2$ dNTP conjugates using cyclic voltammetry with the hanging mercury drop electrode.

Results and discussion

In our previous study [14], anthraquinone-labeled dCTP and 7-deaza-dATP were synthesized and used for DNA labeling via incorporation of corresponding nucleotides into ODNs by DNA polymerases (for general methodologies of this strategy of modified nucleic acids construction, see reviews [2, 17, 28]). Electrochemical measurements revealed the modified ODNs to give well-developed signals due to reversible redox electrochemistry of the AQ moiety. Experiments focused on simultaneous detection of the AQ tags with another type of organic electrochemically active moieties attached to nucleobases in modified ODNs, 3-nitrophenyl [12], indicated possibilities of using the two labels for convenient dual DNA labeling when optimum conditions for their distinction are applied. Namely, conversion of the $PhNO_2$ group into the corresponding hydroxylamine derivative (PhNHOH) via irreversible four-electron reduction of the nitro group facilitated resolution of AQ and $PhNO_2$ signals when anodic responses were measured [14].

Cyclic voltammetry of AQ-dNTP conjugates

Here, we studied in more detail the electrochemical behavior of AQ and $PhNO_2$-labeled dNTPs, **dC^{PAQ}TP**, **dA^{PAQ}TP**, **dC^{PhNO_2}TP**, and **dA^{PhNO_2}TP**. Cyclic voltammograms (CVs) of these four compounds at concentrations of 40 μM, measured in 0.3 M ammonium formate, 0.05 M sodium phosphate, pH 6.9 (a medium optimized for electrochemical analysis of DNA at mercury electrodes, suitable for simultaneous detection of natural electroactive DNA components [1, 3]) without pre-accumulation of the analytes, are presented in Fig. 1. Red curves correspond to CVs measured with initial potential $E_i = 0.0$ V and switching potential $E_{sw} = -0.85$ V, while black dotted curves were obtained for $E_{sw} = -1.85$ V. Both AQ-dNTP conjugates (Fig. 1a, b), when measured with $E_{sw} = -0.85$ V, gave a pair of peaks around −0.4 V corresponding to the reversible anthraquinone/anthrahydroquinone redox system:

$$AQ + 2\ e^- + 2\ H^+ \leftrightarrow\ AQH_2 \qquad (1)$$

The behavior of **dC^{PAQ}TP** (Fig. 1a) was nevertheless in some respects different from that of **dA^{PAQ}TP** (Fig. 1b). First, a considerable difference in the heights of cathodic peak AQ^{red} and anodic peak AQH_2^{ox} (the latter being 3 times higher than the former for 40 μM **dC^{PAQ}TP**; see concentration dependences for further discussion) was observed for **dC^{PAQ}TP**, while for **dA^{PAQ}TP** the intensity of the cathodic peak AQ^{red} was about 3.5-times higher compared to the analogous signal of **dC^{PAQ}TP,** and the anodic peak AQH_2^{ox} of **dA^{PAQ}TP** was higher by only 33 % as compared to the peak AQ^{red} of the same conjugate (Table 1; compare also solid curves in Fig. 2a, where details of the voltammograms are shown). Second, peak-to-peak separation for the AQ/AQH_2 redox process was 19 mV in **dC^{PAQ}TP** and 48 mV in **dA^{PAQ}TP**, suggesting more facile electron transfer in the first instance. Third, for **dA^{PAQ}TP**, clearly developed second pair of peaks at potentials more negative by 27 mV were observed. Differences in the relative intensities of the anodic and cathodic peaks of **dC^{PAQ}TP** and **dA^{PAQ}TP** can be attributed to different adsorbabilities of the two conjugates, with the **dA^{PAQ}TP** adsorbing at the mercury surface more efficiently. The experiment, the results of which is shown in Fig. 2, supports such explanation: when **dC^{PAQ}TP** was allowed to accumulate at the electrode surface with open current circuit for 60 s before the CVs were measured, the height of the peak AQ^{red} increased by about three times. Peak AQH_2^{ox} became significantly higher after pre-accumulation and its height was practically the

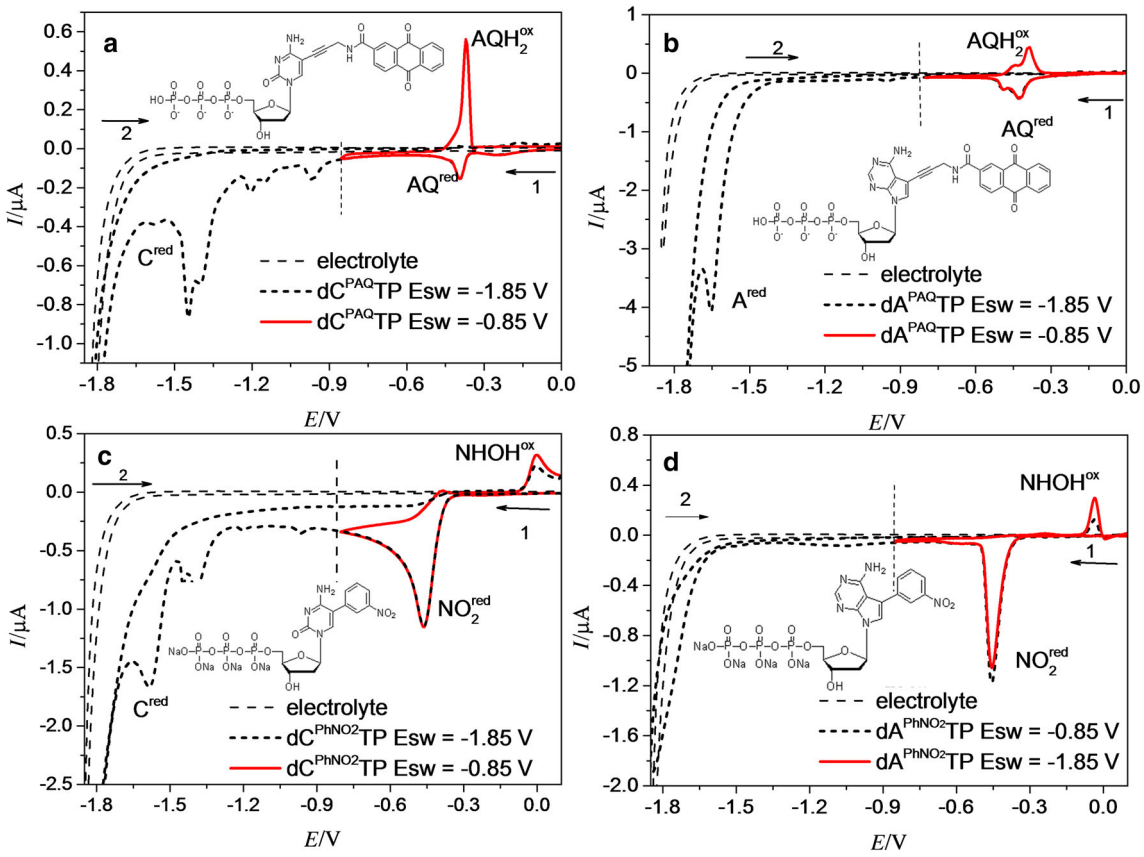

Fig. 1 Cyclic voltammograms of **dC^{PAQ}TP** (**a**), **dA^{PAQ}TP** (**b**), **dC^{PhNO_2}TP** (**c**), and **dA^{PhNO_2}TP** (**d**). Cyclic voltammetry (CV) at HMDE: E_i +0.0 V (**a**, **b**), or +0.1 (**c**, **d**), E_{sw} −1.85 or −0.85 V, scan rate 1 V/s, background electrolyte: 0.3 M ammonium formate, 0.05 M sodium phosphate, pH 6.9, and concentration of all substances was 40 μM

Table 1 Heights and potentials of peaks AQ^{red} and AQH$_2^{ox}$ obtained for dA^{PAQ}TP and dC^{PAQ}TP and of peaks NO$_2^{red}$ and NHOH^{ox} for dA^{PhNO_2}TP and dC^{PhNO_2}TP

Peak	AQ^{red}		AQH$_2^{ox}$	
	Potential/V	Height/μA	Potential/V	Height/μA
dA^{PAQ}TP	−0.428	0.55	−0.380	0.41
dC^{PAQ}TP	−0.394	0.16	−0.375	0.49
Peak	NO$_2^{red}$		NHOH^{ox}	
	Potential/V	Height/μA	Potential/V	Height/μA
dA^{PhNO_2}TP	−0.457	1.01	−0.037	0.31
dC^{PhNO_2}TP	−0.435	2.40	−0.007	0.50

same as the height of the peak AQ^{red}. The **dA^{PAQ}TP** exhibited similar effects upon the accumulation, giving wide cathodic and anodic peaks in which the two reversible pairs (distinguishable in CV measured without accumulation, Fig. 2) were clearly merged.

When the CVs were measured with the $E_{sw} = -1.85$ V (i.e., with a setup previously used in DNA analysis to reduce guanine residues and obtain an anodic peak G of guanine at the mercury electrode [1, 3, 14]), the anodic peak AQH$_2^{ox}$ disappeared in both **dC^{PAQ}TP** and **dA^{PAQ}TP**, suggesting a deeper reduction of the AQ moiety upon applying the highly negative potentials. Blocking of the electrode surface by the reduction products then probably prevents fresh dN^{PAQ}TP from the bulk of solution to give peak AQH$_2^{ox}$ in the anodic scan. The **dC^{PAQ}TP** conjugate (Fig. 1a) exhibited rather complicated behavior in a potential region between −0.9 and −1.7 V, producing several, under the given conditions, irreversible peaks in

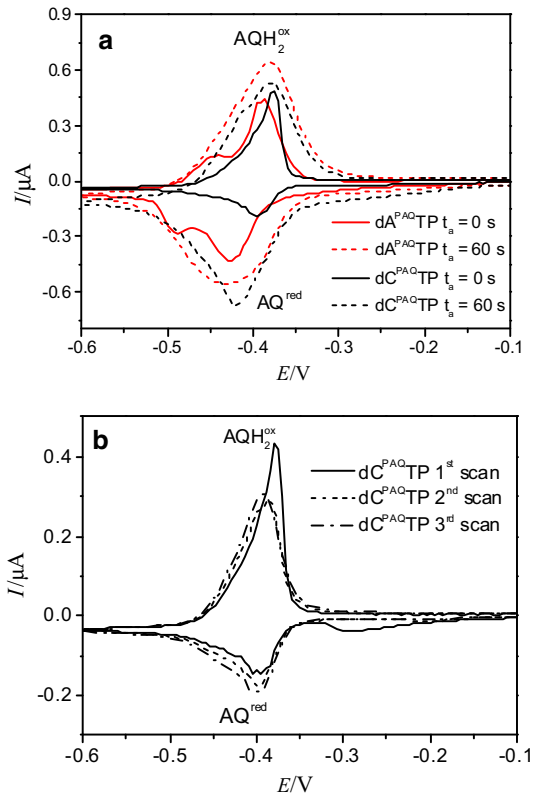

Fig. 2 **a** Effects of adsorptive pre-accumulation (0 or 60 s at open current circuit) on CV responses of **dC^{AQ}TP** and **dA^{PAQ}TP**. **b** Repeated CV scans of **dC^{PAQ}TP** (without pre-accumulation, E_i +0.1 V, E_{sw} −0.6 V, scan rate 1 V/s, and other conditions as in Fig. 1)

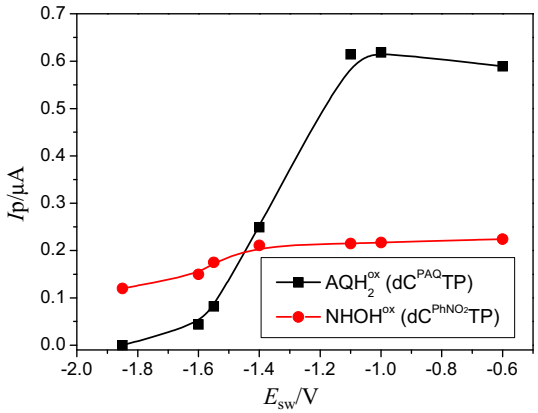

Fig. 3 Dependence of the intensity of peaks AQH_2^{ox} and $NHOH^{ox}$ on switching potential (**dC^{PAQ}TP** and **dC^{PhNO_2}TP**, CV at HMDE, other conditions as in Fig. 1)

the cathodic scan that could be ascribed to reduction processes of ethynyl and carbamoyl groups in the linker, the above proposed reduction of the anthrahydroquinone (see the dependence of peak AQH_2^{ox} height on E_{sw} in Fig. 3, showing a steep decrease of the peak current between −1.1 V and −1.6 V), reduction of cytosine as well as tensammetric processes of the negatively charged dNTPs on the negatively charged surface (note the sharp "spike" at −1.45 V, Fig. 1a). On the contrary, **dA^{PAQ}TP** yielded only one well-developed cathodic peak under the same conditions (peak A^{red}, Fig. 1b), which can be ascribed to reduction of the 7-deazaadenine nucleobase. Differences between the two dNTPs may be due to different adsorption modes (see above), influencing availability of different electroreducible groups for electronic communication with the electrode. Taken together, the shapes of CVs of individual PAQ conjugates, as well as differences observed between **dC^{PAQ}TP** and **dA^{PAQ}TP** both in the region of the AQ reversible electrochemistry and in the more negative potential region, suggest rather complicated processes undergone by these complex compounds on the mercury electrode surface (see also discussion of concentration dependences below).

Cyclic voltammetry of $PhNO_2$-dNTP conjugates

Both nitrophenyl-labeled dNTPs, **dC^{PhNO_2}TP** (Fig. 1c) and **dA^{PhNO_2}TP** (Fig. 1d), gave an irreversible cathodic signal, peak NO_2^{red}, around −0.45 V (Table 1). Nitro group is known to be electrochemically reduced at various types of electrodes [29, 30] to hydroxylamine:

$$-NO_2 + 4\ e^- + 4\ H^+ - H_2O \rightarrow -NH\text{-}OH \qquad (2)$$

Due to the involvement of four electrons, the latter electrode reaction gives rise to a strong reduction signal allowing sensitive polarographic or voltammetric determination of various nitro compounds [31–39], including environmental pollutants [40–44]. In several proof-of-concept applications it has been utilized for convenient DNA labeling as well [8, 9, 12, 14]. The hydroxylamime moiety resulting from (2) is reversibly oxidizable by two electrons to the nitroso group [30]:

$$-NH\text{-}OH - 2\ e^- - 2\ H^+ \leftrightarrow NO \qquad (3)$$

Hydroxylamine reduction is reflected in anodic signals (peak $NHOH^{ox}$) yielded by both $PhNO_2$ dNTP conjugates close to 0.0 V (Fig. 1c, d; Table 1). In contrast to the anodic peak AQH_2^{ox}, the peak $NHOH^{ox}$ was observed on the CVs even when the measurements were performed with $E_{sw} = -1.85$ V, displaying only partial decrease of its intensity. Dependence of the peak $NHOH^{ox}$ height on E_{sw}, measured for **dC^{PhNO_2}TP** (Fig. 3), shows the peak current to be practically unchanged between $E_{sw} = -0.6$ V and −1.4, and to decrease gradually with E_{sw} being shifted to more negative potentials; for $E_{sw} = -1.85$ V the peak $NHOH^{ox}$ height corresponded to 55 % of value measured with $E_{sw} = -0.6$ V. Such behavior suggests that either the corresponding redox moiety is not destroyed upon the electrode polarization to highly negative potentials, or the

electrode surface does not get fully blocked by reduction products and the anodic peak $NHOH^{ox}$ is produced by fresh analyte from the bulk of solution. Since the peak $NHOH^{ox}$ measured with $PhNO_2$-labeled ODN using *ex situ* voltammetric procedure (i.e., with adsorbed layer onto the electrode and no analyte present in the bulk of background electrolyte) completely disappeared for $E_{sw} = -1.2$ V (not shown preliminary data; a complex study with labeled ODNs will be published elsewhere), the explanation based on involvement of fresh $dN^{PhNO_2}TP$ from solution appears to be more likely. Notably, significant decrease of the $NHOH^{ox}$ height in **$dC^{PhNO_2}TP$** was observed at E_{sw} values coinciding with potential of reduction of the cytosine nucleobase (Fig. 1c), and partial electrode blocking with products of the latter reaction could cause the observed decrease of the peak $NHOH^{ox}$ intensity. Similarly as in the case of corresponding AQ conjugates (Fig. 1a, b), **$dA^{PhNO_2}TP$** differed from **$dC^{PhNO_2}TP$** by absence of any distinct signals in the potential region between −0.6 and −1.85 V (Fig. 1d). The **$dA^{PhNO_2}TP$** did not yield even the signal of 7-deazaadenine reduction in the ammonium formate medium (it was nevertheless observed in Britton–Robinson buffer at pH ≤ 6, see below). On the other hand, the behavior of **$dC^{PhNO2}TP$** in the same potential region was similar to that of **$dC^{PAQ}TP$**, suggesting the nucleobase to be a critical component of the dNTP conjugate that dictates its behavior on the negatively charged mercury surface.

Effects of dNTP concentration, pH of background electrolyte, and scan rate

Dependences of intensities of peaks AQ^{red}/AQH_2^{ox} measured without pre-accumulation for **$dC^{PAQ}TP$** and **$dA^{PAQ}TP$**, and of peaks NO_2^{red} and $NHOH^{ox}$ measured under the same conditions with **$dA^{PhNO_2}TP$**, are shown in Fig. 4. The height of the cathodic peak AQ^{red} of **$dC^{PAQ}TP$** increased more or less linearly within the concentration region between 0 and 80 μM (Fig. 4a). A strikingly different concentration dependence was observed for the anodic peak AQH_2^{ox} of the same dNTP conjugate. At low concentrations up to 25 μM **$dC^{PAQ}TP$**, both peaks AQ^{red} and AQH_2^{ox} followed an identical trend. However, between 25 and 40 μM **$dC^{PAQ}TP$**, the height of peak AQH_2^{ox} increased steeply, reached its maximum at 50 μM **$dC^{PAQ}TP$** and then gradually decreased. The sigmoidal shape of the concentration dependence suggests intermolecular interactions at the electrode surface: the steep increase of the signal around 30 μM **$dC^{PAQ}TP$** can be explained by positive cooperative effects of the already adsorbed (and electrochemically reduced) molecules of μM **$dC^{PAQ}TP$** on adsorption of more molecules from the solution taking place from a critical surface coverage (i.e., distances

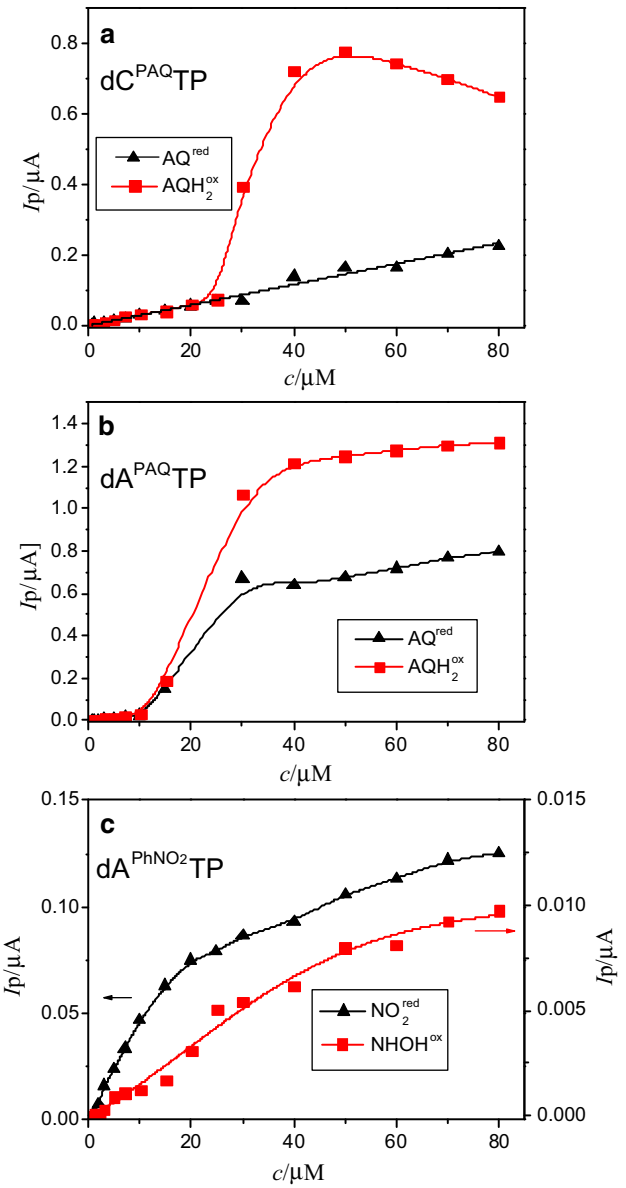

Fig. 4 Dependence of the intensity of peaks AQ^{red}, AQH_2^{ox}, NO_2^{red}, and $NHOH^{ox}$ on dNTP concentration: **a $dC^{PAQ}TP$**, **b $dA^{PAQ}TP$**, and **c $dA^{PhNO_2}TP$** (E_{sw} −0.85 V and other conditions as in Fig. 1)

between molecules at the surface), which under the given conditions is dictated by solution concentration of the **$dC^{PAQ}TP$**. Alternatively, the reduction of **$dC^{PAQ}TP$** may be accompanied by the formation of an ordered structure of the adsorbed layer and orientation of the AQH_2 in a way facilitating the oxidation process. Since the cooperative effect was reflected in peak AQH_2^{ox}, but not AQ^{red} heights, the presumptive intermolecular interactions were specific, in the case of **$dC^{PAQ}TP$**, for its reduced form. Moreover, differences in the peak AQ^{red} and AQH_2^{ox} intensities measured for 40 μM **$dC^{PAQ}TP$** were retained in repeated CV scans (Fig. 2b), suggesting the presumptive interaction to be reversibly on/off switchable via changing the AQ

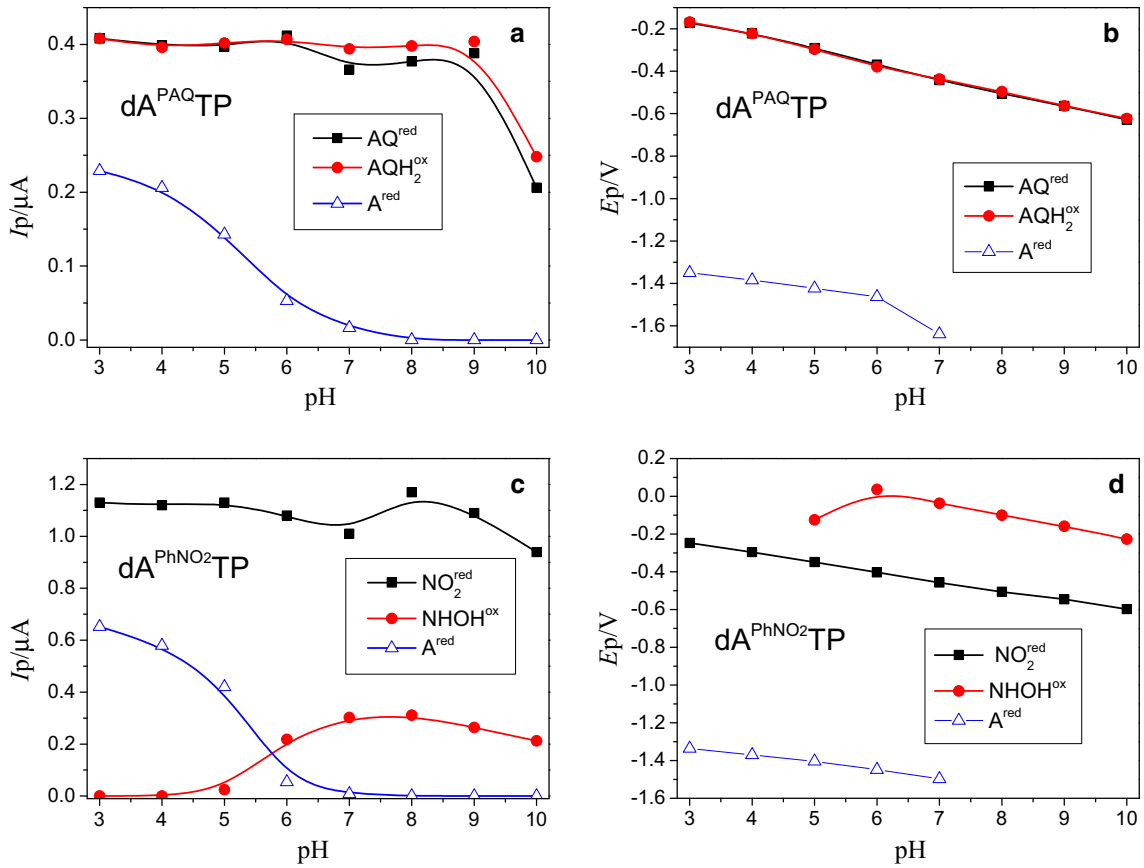

Fig. 5 Dependence of the intensity (**a**) and potential (**b**) of peaks AQ^{red}, AQH_2^{ox}, and A^{red} for **dA^{PAQ}TP** and intensity (**c**) and potential (**d**) of peaks NO_2^{red}, $NHOH^{ox}$, and A^{red} of **dA^{PhNO_2}TP** on pH of background electrolyte (E_{sw} −0.85 V, scan rate 1 V/s, background electrolyte: Britton–Robinson buffers of the given pH and other conditions as in Fig. 1)

redox state. In contrast to **dC^{PAQ}TP**, for **dA^{PAQ}TP** the S-shaped dependences of signal intensity were obtained for both cathodic and anodic peaks, indicating that analogous intermolecular interactions may have occurred in both reduced and oxidized forms of the latter conjugate, facilitating accumulation of the oxidized form at the electrode surface (see above). Concentration dependence of the **dA^{PhNO2}TP** peak NO_2^{red} (Fig. 4c) involved a linear region between 0 and 10 μM, followed by a less steeply increasing part at higher concentration. Dependence of the height of peak $NHOH^{ox}$ exhibited certain sign of transition around 20 μM; nevertheless, compared to signals of the AQ conjugates this effect was poorly pronounced.

Dependences of heights and potentials of signals yielded by **dA^{PAQ}TP** and **dA^{PhNO2}TP** on pH of the background electrolyte, measured in Britton–Robinson buffer, are shown in Fig. 5. The heights of peaks AQ^{red} and AQH_2^{ox} were almost pH-independent in a wide range between pH 3 and 9 (Fig. 5a), indicating that the availability of protons were not limiting for reaction (1) to take place under the given conditions. A similar behavior was observed for peak NO_2^{red} of **dA^{PhNO2}TP** (Fig. 5c). By contrast, peak $NHOH^{ox}$ was detectable only in pH > 5 (Fig. 5c), most probably due to reduction of the hydroxylamine to amine that took place in the acidic media (indeed, an additional pH-dependent cathodic peak was detected in pH ≤ 5, but not in pH above 5; not shown). In both conjugates, peak A^{red} due to reduction of the nucleobase was observed only in pH ≤ 6, in agreement with earlier data showing that protonation was a prerequisite for the nucleobase reduction at the mercury electrode (reviewed in [3]). The potentials of all measured signals shifted to more negative potentials with increasing pH, exhibiting almost parallel trends (Fig. 5b, d).

The effects of scan rate were studied in the ammonium formate medium and the results obtained for **dC^{PAQ}TP** and **dC^{PhNO2}TP** are displayed in Fig. 6. As could be expected for rather complex molecules of the dNTP conjugates, involving hydrophobic, hydrophilic, and/or negatively charged parts, dependences of the measured signals on scan rate mostly did not fit into simple models valid for electrode processes driven by either diffusion or adsorption. Peak NO_2^{red} of **dC^{PhNO2}TP** followed a slightly concave dependence on the scan rate (growing less steeply than a linear function, Fig. 6b); when the peak heights were

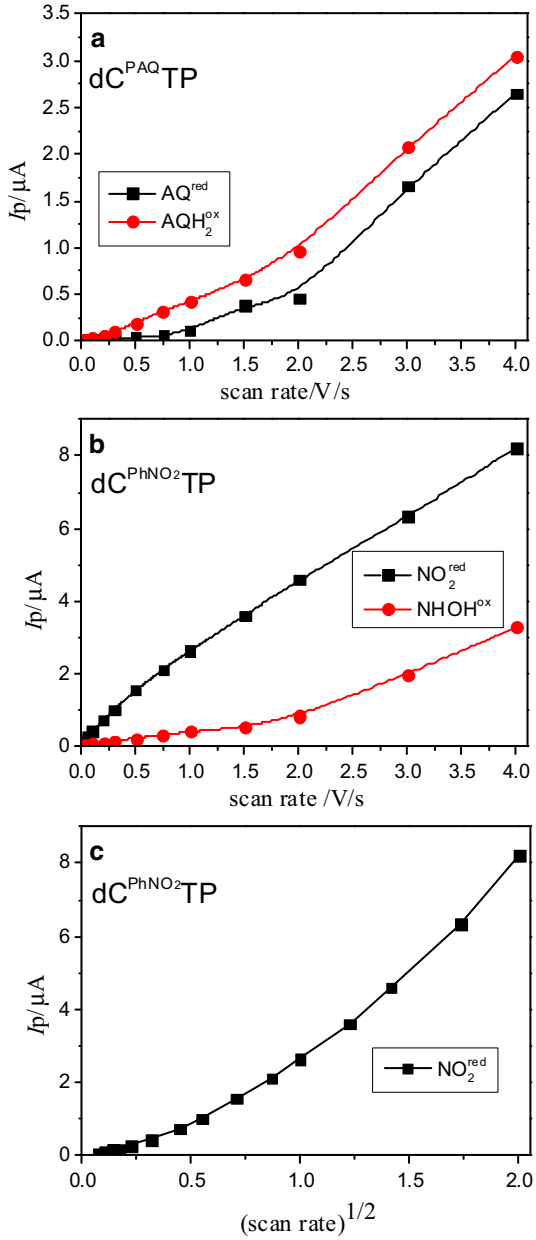

Fig. 6 Dependence of intensity of peaks AQ^{red}, AQH_2^{ox} NO_2^{red}, and $NHOH^{ox}$ on scan rate for **dC^{PAQ}TP** (**a**) and **dC^{PhNO2}TP** (**b**); dependence of peak NO_2^{red} on square root of scan rate for **dC^{PhNO2}TP** (**c**) (E_{sw} −0.85 V, other conditions as in Fig. 1)

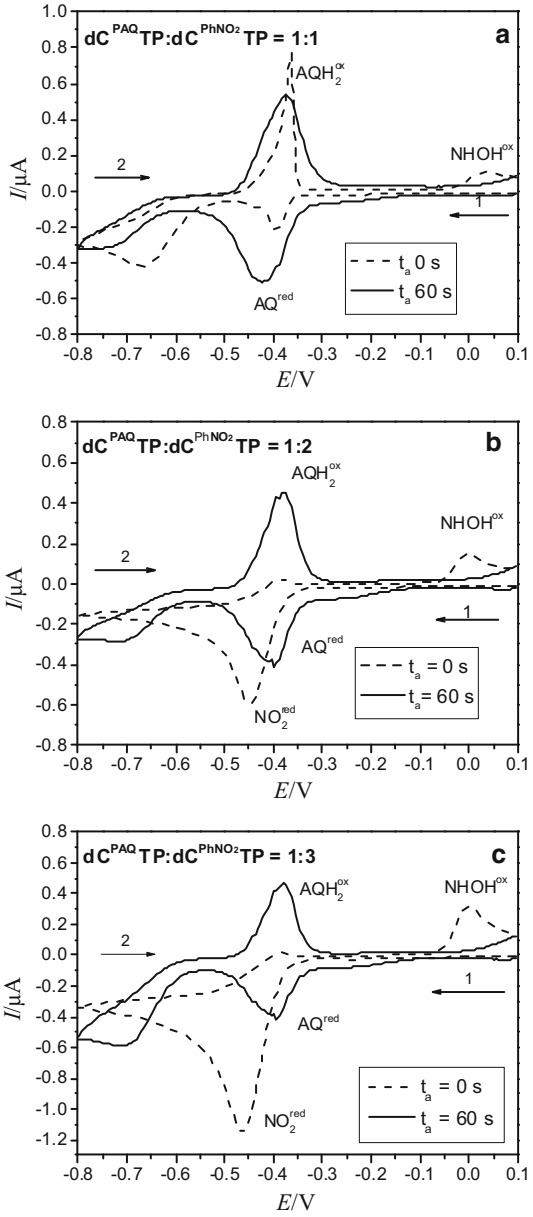

Fig. 7 Voltammetric responses of mixtures of **dC^{PAQ}TP** and **dC^{PhNO2}TP** at various ratios: **a dC^{PAQ}TP:dC^{PhNO2}TP** = 1:1, **b dC^{PAQ}TP:dC^{PhNO2}TP** = 1:2, **c dC^{PAQ}TP:dC^{PhNO2}TP** = 1:3, accumulation time 0 s (dashed) or 60 s (solid; E_{sw} −0.85 V, scan rate 1 V/s, and other conditions as in Fig. 1)

plotted against square root of the scan rate (Fig. 6c), the resulting dependence was significantly convex (increasing more steeply than a line), together indicating the combined effects of diffusion and strong adsorption. The other peaks, AQ^{red} and AQH_2^{ox} of **dC^{PAQ}TP** and $NHOH^{ox}$ of **dC^{PhNO2}TP,** exhibited strongly supralinear dependences of their heights on scan rate, suggesting more complex process possibly involving time-dependent desorption/reorientation of the dNTP molecules at the negatively charged surface or the above discussed lateral interactions of the AQ conjugates at the electrode surface.

Mixtures of AQ- and $PhNO_2$-labeled dNTPs

Finally, we have been interested in the possibility of simultaneous voltammetric detection of the AQ- and $PhNO_2$-labeled dNTPs in mixtures (Fig. 7). For this purpose, **dC^{PAQ}TP** and **C^{PhNO2}TP** were mixed at ratios 1:1, 1:2,

and 1:3 (keeping the **dC^{PAQ}TP** concentration constant at 20 μM), and CVs were measured without pre-accumulation (dashed lines in Fig. 7) or after a 60-s pre-accumulation (solid lines). The results of these experiments demonstrated the above discussed preferential accumulation of the AQ conjugate at the electrode surface. When the CVs were measured without the pre-accumulation, peak NHOH^{ox} was detectable at the dNTPs ratio 1:1, but not the peak NO_2, the potential of which (about −0.45 V) was close to the potential of AQ reduction. Upon increasing the **C^{PhNO2}TP/dC^{PAQ}TP** ratio to 2:1 and 3:1, the peak NO_2 was unmasked and peaks of the AQ^{red}/AQH_2^{ox} depressed. However, after the pre-accumulation, both signals of **C^{PhNO2}TP**, peak NO_2^{red}, and peak NHOH^{ox}, were strongly depressed even in threefold excess of the latter dNTP, suggesting that the more strongly adsorbing **dC^{PAQ}TP** displaced the **C^{PhNO2}TP** from the electrode surface. Interestingly, in the presence of both conjugates, a new cathodic peak appeared around −0.65 V (well developed, at the **C^{PhNO2}TP/dC^{PAQ}TP** ratio of 1:1 when the measurement was performed without pre-accumulation (Fig. 7a), and in measurements with pre-accumulation its intensity exhibited increasing trend with increasing concentration of **C^{PhNO2}TP**). This signal may indicate a chemical reaction between products or intermediate of electrochemical reduction of AQ and the nitro group at the electrode surface.

Conclusions

Cytosine or 7-deazaadenine dNTPs modified at the base residue with electrochemically active anthraquinone or 3-nitrophenyl moieties were studied using cyclic voltammetry with the hanging mercury drop electrode. AQ moiety in the dNTP conjugates is shown to retain its well-pronounced reversible electrochemistry around −0.40 V. The nitro group in $PhNO_2$ exhibits characteristic irreversible reduction around −0.45 V. The product of this reduction, phenylhydroxylamine (NHOH), gives a well-developed signal close to 0.0 V due its reversible oxidation to the corresponding nitroso compound. Further electrochemical reduction of the AQH_2 and NHOH redox groups can be used for their selective switching off, depending on the potential applied and composition of the background electrolyte (namely, in acidic media the signal of NHOH oxidation disappeared, suggesting irreversible reduction of the hydroxylamine to amine). The modified dNTPs studied differed in their adsorbability at the mercury electrode surface. In general, the tendency to being accumulated at the electrode was higher in AQ-modified dNTPs than in the $PhNO_2$ derivatives, and among the former **dA^{AQ}TP** was more efficiently adsorbed in its oxidized (AQ) form than **dC^{AQ}TP**. The shapes of concentration dependences indicate intermolecular interactions of the AQ conjugates at the electrode surface that appear to be redox sensitive (specific for the reduced AQH_2 form) in **dC^{AQ}TP**. In our follow-up study (research in progress), the electrochemical properties of oligonucleotides modified with AQ- and $PhNO_2$ conjugates are investigated and the possibilities of the analytical utilization of specific properties of the two types of DNA labels are tested (results will be published elsewhere).

Experimental

Synthesis of anthraquinone- and 3-nitrophenyl-labeled deoxynucleoside triphosphates

Anthraquinone-modified nucleoside triphosphates (dNTPs) bearing anthraquinone attached through a propargylcarbamoyl linker at the 5-position of cytosine (**dC^{PAQ}TP**) or at the 7-position of 7-deazaadenine (**dA^{PAQ}TP**) were prepared by Sonogashira cross-coupling of corresponding halogenated dNTPs with 2-(2-propynylcarbamoyl)anthraquinone according to [14]. Analogous 3-nitrophenyl-modified dNTPs were prepared by the Suzuki–Miyaura reaction of 7-iodo-7-deaza-2′-dATP (to obtain **dA^{PhNO2}TP**) or 5-iodo-2′-deoxycytidine 5′-dCTP (to obtain **dC^{PhNO2}TP**) with 3-nitrophenylboronic acid according to [12]. Both modified dNTPs were kindly donated by Prof. Michal Hocek.

Electrochemical analysis

Nucleoside triphosphates were analyzed by conventional in situ CV with a hanging mercury drop electrode. CV settings: scan rate 1 V/s, initial potential 0.0 V or +0.1 V, switching potentials −0.85 or −1.85 V. Background electrolyte: 0.3 M ammonium formate, 0.05 mM sodium phosphate, pH 6.9, if not stated otherwise. All measurements were performed at room temperature by using an Autolab analyzer (Eco Chemie, The Netherlands) in connection with VA-stand 663 (Metrohm, Herisau, Switzerland). The three-electrode system was used with an Ag|AgCl|3 M KCl electrode as a reference and platinum wire as an auxiliary electrode. Measurements were performed after deaeration of the solution by argon purging.

Acknowledgments This work was supported by the Czech Science Foundation (grant P206/12/G151 to M.F. and 206/12/2378 to L.H.) and by the ASCR (RVO 68081707). The authors thank Jana Balintová, Hana Macíčková-Cahová, and Michal Hocek (Institute of Organic Chemistry and Biochemistry, ASCR, Prague, Czech

Republic) for providing the modified nucleoside triphosphates used in this study.

References

1. Fojta M, Jelen F, Havran L, Palecek E (2008) Curr Anal Chem 4:250
2. Hocek M, Fojta M (2011) Chem Soc Rev 40:5802
3. Palecek E, Bartosik M (2012) Chem Rev 112:3427
4. Fojta M, Kostecka P, Pivonkova H, Horakova P, Havran L (2011) Curr Anal Chem 7:35
5. Bartosik M, Trefulka M, Hrstka R, Vojtesek B, Palecek E (2013) Electrochem Commun 33:55
6. Dziuba D, Pohl R, Hocek M (2014) Bioconjugate Chem 1984
7. Riedl J, Pohl R, Ernsting NP, Orsag P, Fojta M, Hocek M (2012) Chem Sci 3:2797
8. Balintova J, Spacek J, Pohl R, Brazdova M, Havran L, Fojta M, Hocek M (2014) Chem Sci 6:575
9. Raindlova V, Pohl R, Klepetarova B, Havran L, Simkova E, Horakova P, Pivonkova H, Fojta M, Hocek M (2012) ChemPlusChem 77:652
10. Dadova J, Orsag P, Pohl R, Brazdova M, Fojta M, Hocek M (2013) Angew Chem Int Ed 52:10515
11. Brazdilova P, Vrabel M, Pohl R, Pivonkova H, Havran L, Hocek M, Fojta M (2007) Chem Eur J 13:9527
12. Cahova H, Havran L, Brazdilova P, Pivonkova H, Pohl R, Fojta M, Hocek M (2008) Angew Chem Int Ed 47:2059
13. Vrabel M, Horakova P, Pivonkova H, Kalachova L, Cernocka H, Cahova H, Pohl R, Sebest P, Havran L, Hocek M, Fojta M (2009) Chem Eur J 15:1144
14. Balintova J, Pohl R, Horakova P, Vidlakova P, Havran L, Fojta M, Hocek M (2011) Chem Eur J 17:14063
15. Balintova J, Plucnara M, Vidlakova P, Pohl R, Havran L, Fojta M, Hocek M (2013) Chem Eur J 19:12720
16. Simonova A, Balintova J, Pohl R, Havran L, Fojta M, Hocek M (2014) ChemPlusChem 79:1703
17. Hocek M (2014) J Org Chem 79:9914
18. Fojta M, Kostecka P, Trefulka MR, Havran L, Palecek E (2007) Anal Chem 79:1022
19. Ajloo D, Yoonesi B, Soleymanpour A (2010) Int J Electrochem Sci 5:459
20. Batchelor-McAuley C, Li Q, Dapin SM, Compton RG (2010) J Phys Chem B 114:4094
21. Quan M, Sanchez D, Wasylkiw MF, Smith DK (2007) J Am Chem Soc 129:12847
22. Mahajan S, Richardson J, Ben Gaied N, Zhao Z, Brown T, Bartlett PN (2009) Electroanalysis 21:2190
23. Wettig SD, Bare GA, Skinner RJS, Lee JS (2003) Nano Lett 3:617
24. Zhang Y-J, He X-P, Hu M, Li Z, Shi X-X, Chen G-R (2011) Dyes Pigm 88:391
25. Abou-Elkhair RAI, Dixon DW, Netzel TL (2009) J Org Chem 74:4712
26. Gorodetsky AA, Barton JK (2007) J Am Chem Soc 129:6074
27. Jacobsen MF, Ferapontova EE, Gothelf KV (2009) Org Biomol Chem 7:905
28. Hocek M, Fojta M (2008) Org Biomol Chem 6:2233
29. Peckova K, Barek J, Navratil T, Yosypchuk B, Zima J (2009) Anal Lett 42:2339
30. Zuman P (1993) Collect Czech Chem Commun 58:41
31. Beckett EL, Lawrence NS, Davis J, Compton RG (2002) Anal Lett 35:339
32. Boateng A, Brajter-Toth A (2012) Analyst 137:4531
33. Cordero-Rando MD, Barea-Zamora M, Barbera-Salvador JM, Naranjo-Rodriguez I, Munoz-Leyva JA, de Cisneros J (1999) Mikrochim Acta 132:7
34. De Souza D, Mascaro LH, Fatibello-Filho O (2011) Int J Anal Chem 2011:726462
35. Gupta S, Agarwal H, Gupta M, Verma PS (2010) J Indian Chem Soc 87:481
36. Gupta S, Gupta M, Verma PS (2009) Asian J Chem 21:7316
37. Chu L, Han L, Zhang X (2011) J Appl Electrochem 41:687
38. Kawde A-N, Aziz MA (2014) Electroanalysis 26:2484
39. Liu Z, Zhang H, Ma H, Hou S (2011) Electroanalysis 23:2851
40. Danhel A, Peckova K, Cizek K, Barek J, Zima J, Yosypchuk B, Navratil T (2007) Chem List 101:144
41. Dejmkova H, Stoica A-I, Barek J, Zima J (2011) Talanta 85:2594
42. Deylova D, Yosypchuk B, Vyskocil V, Barek J (2011) Electroanalysis 23:1548
43. Fischer J, Vanourkova L, Danhel A, Vyskocil V, Cizek K, Barek J, Peckova K, Yosypchuk B, Navratil T (2007) Int J Electrochem Sci 2:226
44. Niaz A, Fischer J, Barek J, Yosypchuk B, Sirajuddin, Bhanger MI (2009) Electroanalysis 21:1786